UCRL-21005
SAND 616-007

CORROSION TESTING OF TYPE 304L STAINLESS STEEL IN TUFF GROUNDWATER ENVIRONMENTS

R. E. Westerman
S. G. Pitman
J. H. Haberman

Work Performed at
Pacific Northwest Laboratory
Richland, WA 99352

November 1987

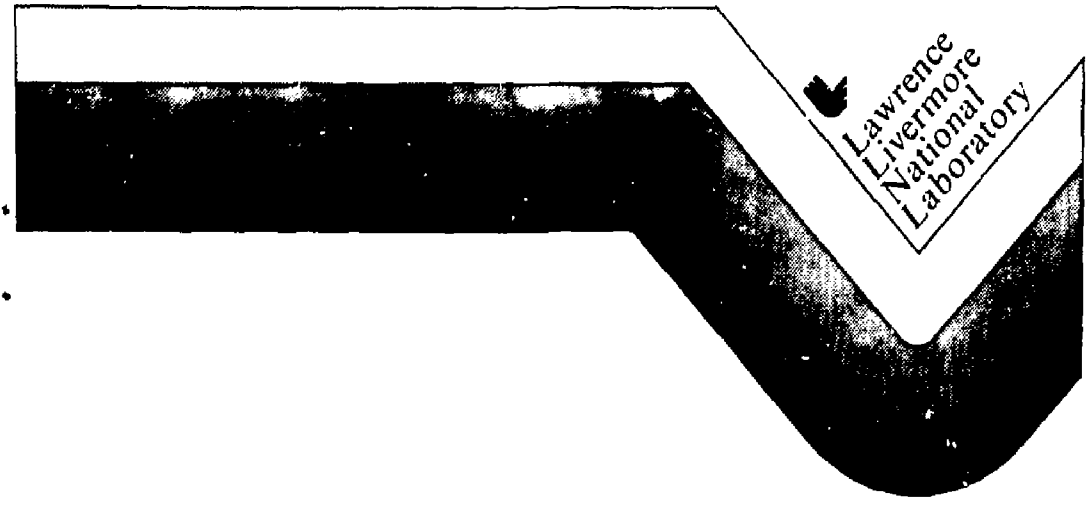

Prepared by Nevada Nuclear Waste Storage Investigations (NNWSI) Project participants as part of the Civilian Radioactive Waste Management Program. The NNWSI Project is managed by the Waste Management Project Office of the U.S. Department of Energy, Nevada Operations Office. NNWSI Project work is sponsored by the Office of Geologic Repositories of the DOE Office of Civilian Radioactive Waste Management.

UCRL--21005

DE88 006242

CORROSION TESTING OF TYPE 304L STAINLESS STEEL IN TUFF GROUNDWATER ENVIRONMENTS

R. E. Westerman
S. G. Pitman
J. H. Haberman

PNL-5829

Work Performed at
Pacific Northwest Laboratory
Richland, WA 99352

November 1987

CONTENTS

FIGURES

TABLES

1.0 INTRODUCTION

The Department of Energy's Nevada Nuclear Waste Storage Investigation (NNWSI) Project is evaluating the suitability of the Topopah Spring Member of the Paintbrush Tuff (Tpt) at Yucca Mountain, Nevada, as a repository site for high-level nuclear waste disposal. The target horizon is located at a depth of 350 to 400 m, approximately 200 to 400 m above the water table. In order for a waste package to fulfill the long-term containment requirements imposed by the Nuclear Regulatory Commission Regulation 10 CFR 60, it may be necessary for the waste package containers to resist failure by several different degradation modes--such as general corrosion, pitting and crevice corrosion, stress-corrosion cracking (SCC), hydrogen embrittlement, aging reactions, and mechanical overload--for up to 1000 years. It is estimated that the majority of the packages in the tuff repository, and the rock within 1 m of the waste packages, would remain above the boiling point for approximately 300 years (Glassley 1986). Thus, the containers will initially be exposed to irradiated water vapor and atmospheric gases at elevated temperature. Eventually, after the containment period for most of the packages, the container temperature will drop below the boiling point of water, thus allowing liquid water to contact the waste containers if it is present. For anticipated conditions, the majority of containers will not come in contact with liquid water.

Emplacement of waste packages in the tuff repository will cause physical and chemical changes in the rock adjacent to the emplacement boreholes. These are primarily the result of the thermal and radiation fields generated by the waste forms within the containers. The decay of radionuclides transfers kinetic energy to the decay products, and collision of these decay products with the surrounding materials converts this energy into heat, increasing the temperature. The dissipation of the decay product kinetic energy is referred to as the power output of the waste form. For any high-level waste form, the power output is highest when the waste is newest; it decreases as the radionuclides decay to nonradioactive nuclei. Many of the fission products present in spent fuel and reprocessed waste have relatively short half-lives. As a result, the power output of the waste will decrease rather rapidly during the first few decades of storage (O'Neal et al. 1984).

Immediately after waste package emplacement, the temperature of the rock and its associated pore water will increase; as this occurs, water will be driven away from the waste package. When the rock temperature rises above about 96°C (estimated boiling point at horizon elevation in Yucca Mountain), most of the liquid water in the rock will vaporize. The atmosphere in the pore spaces and around the waste packages will then consist of a mixture of air and steam. As the rock cools below 96°C, liquid water will slowly migrate back into the rock pores. Resaturation of the rock around defense waste packages may require hundreds of years; in the case of spent fuel packages, resaturation may take thousands of years (O'Neal et al. 1984).

The composition of the pore water in the repository horizon is unknown. Available evidence suggests that the pore water composition will be similar to that obtainable from well J-13 (Glassley 1986), since the producing horizon of this well is the Topopah Spring tuff. The composition of water from well J-13 is low in dissolved cations and anions, including bicarbonate (2.34 m mol/L) and chloride (0.18 m mol/L). The pH of this water is nearly neutral (pH=6.9).

Vaporization of the pore water during the thermal perturbation of the environment will result in the deposition of some salts in the pore spaces. When the waste package environment cools to temperatures that will allow the presence of liquid water, the salts will be redissolved if liquid water does return. Migration of this water to the vicinity of the waste package may occur, thus providing a potential for water of a composition different from that of J-13 to contact the container. Because the relative and absolute volumes of salts that will be present in the waste package environment are small, it is unlikely that high ionic strength solutions will contact the waste package via the mechanism. It is nevertheless necessary to evaluate the effects of higher ionic strength solutions on container material performance in order to understand the consequences of scenarios in which dilute solutions drip onto a hot container and evaporate, depositing salts in the process.

To determine the extent to which such environmental conditions could contribute to failure of Type 304L stainless steel (SS) by SCC was the principal motivation for the present study, performed at Pacific Northwest Laboratory

(PNL).[a] Type 304L SS is expected to have excellent general corrosion resistance in air and steam at temperatures in the range from 95 to 300°C and in non-saline, near-neutral-pH waters below 95°C. Water from the J-13 well exhibits these characteristics. A conservative estimate of the wastage of 304L SS during the containment period (up to 1000 years) indicates a loss of 0.1 cm from a 1-cm-thick canister wall. This estimate was based on "high values" of uniform corrosion and oxidation rates in water, steam, and air (LaQue and Copson 1963) and on assumed linear oxide growth kinetics (McCright et al. 1983).

The conditions that limit the use of 304L SS are rarely general corrosion wastage, but rather occur by much more rapid penetration via localized or stress-assisted forms of corrosion. The primary goal of the experimental test plan is therefore to determine the extent to which these forms of corrosion could occur during the containment period. For purposes of organization, the localized/stress forms of corrosion can be categorized as follows:

1. Corrosion forms favored by a sensitized microstructure - Such a microstructure can develop during the fabrication and welding of the container, or at relatively low temperatures during storage in the repository at container surface temperatures in excess of about 250°C. The sensitized microstructure may lead to intergranular corrosion or intergranular stress-corrosion cracking (IGSCC) because of the expected oxidizing nature of the aqueous environment, should it come in contact with the container surface.

2. Corrosion forms favored by concentration of the different chemical species in J-13 water - The chloride-ion concentration is of paramount concern with regard to resistance of stainless steels to localized and stress-assisted forms of corrosion. The other ions present in J-13 water may favor or retard these kinds of corrosion attack. Pitting attack, crevice attack, and transgranular stress-corrosion cracking (TGSCC) are forms of corrosion that can develop on 304L in

(a) Operated for the U.S. Department of Energy (DOE) by Battelle Memorial Institute.

concentrated electrolytes--particularly in high-chloride solutions (McCright et al. 1983). A number of possible concentrating mechanisms may operate in a waste repository. Concentration of the cracking species is considered the most serious threat to the integrity of waste packages with respect to SCC (Beavers et al. 1985).

The ultimate purpose of the work was to add to the data base that will eventually be used to determine whether or not 304L SS is a suitable material for a waste package container, or whether recourse will have to be made to materials, such as 316 L SS or alloy 825, which are more resistant to SCC and localized corrosion.

Although the testing of 304L SS was emphasized in the present study, specimens of 304 SS were included throughout the work to assist in ascertaining the severity of the tests to which the 304L SS material was being subjected. Limited tests on 316L SS material were also included as an adjunct to the slow-strain-rate (SSR) test matrix to determine the potential effect of certain sensitization heat treatments on its behavior.

2.0 TECHNICAL APPROACH

The SCC susceptibility of 304L SS was determined by three testing methods in the present study. Irradiation-corrosion, boildown, and SSR testing methods are described. The relatively severe test conditions used in this study, including mechanical stresses, solute concentrations, and irradiation rates, were chosen to provide conservative tests for determining susceptibility to SCC.

2.1 IRRADIATION-CORROSION TESTS

The surfaces of the waste packages in a repository located in tuff in the unsaturated zone are expected to be exposed ultimately to vadose water or to residues from the evaporation of vadose water, as modified by gamma irradiation from the waste form. As it is extremely difficult to predict *a priori* the effect that products of groundwater radiolysis (such as peroxides) might have on the SCC resistance of a stressed stainless steel, it is essential that actual experimental studies be performed under irradiated conditions. The irradiation-corrosion testing portion of the present study involved exposure of U-bend specimens to ^{60}Co-irradiated air/groundwater environments at elevated temperatures for protracted time periods. Any cracking of a U-bend specimen was defined as specimen failure and indicated susceptibility to SCC under those environmental conditions. It should be noted that both the stress in the specimens and the gamma ray dose rates were in excess of anticipated conditions in the repository. To be specific, after about 300 years, when the temperature may decrease below the boiling point, the gamma flux is expected to be on the order of only 10^2 to 10^3 R/h.

2.2 BOILDOWN TEST

A waste package emplaced in a tuff repository in the unsaturated zone is expected to eventually cool to the point where vadose water can contact its surface. Dissolved species could become more concentrated either by initial evaporation of the water in a mass of rock, leaving behind species that could

later be redissolved in a smaller volume of water, or by direct impingement of water onto hot package surfaces, resulting in distillation and deposition of solutes.

Such solutes, especially halides, could promote the SCC of austenitic steels, especially under the elevated-temperature, oxidizing conditions expected in the repository. A boildown test was therefore conducted in which U-bend specimens were embedded in water-saturated tuff rock fragments. Regular boildowns of the water (and subsequent replacement with fresh groundwater) were intended to simulate the solute concentration phenomenon that might take place on waste package surfaces. Any U-bend specimen cracking observed at the time of specimen examination was taken to signal some degree of SCC sensitivity to the environment.

The testing of 304 SS and 304L SS was emphasized in this study. The 304L SS represented the current reference waste package container material; the 304 SS was primarily included as a "standard" by which to gauge the severity of the test.

2.3 SLOW-STRAIN-RATE TESTS

A major portion of the present study was devoted to determining the behavior of stainless steels under SSR testing conditions in nonirradiated environments of tuff groundwater. In the SSR test, a specimen is typically loaded in the service environment and strained until failure occurs. A range of (low) displacement rates is often used so that the strain rate effects can be investigated. The continual straining of the specimen in tension increases its surface area and continually breaks the oxide surface film to expose unoxidized material, which can provide active sites for environment/metal interactions.

An SSR test can indicate the susceptibility of metals to environmentally enhanced cracking in three ways (Payer et al. 1976):

1. loss of ductility relative to an inert environment
2. ductility diminution at a particular strain rate relative to other strain rates
3. fractographic evidence of brittle failure.

3.0 MATERIALS

The materials used in the corrosion tests are described in this section.

3.1 METALS

Sheet stock, 1.52 mm (0.060 in.) thick, of 304 and 304L SS was obtained for the fabrication of U-bend specimens. Plate stock, 6.35 mm (0.25 in.) thick, of 304 and 304L SS was obtained for fabrication of SSR test specimens. In addition, SSR specimens of 316L SS were obtained directly from Lawrence Livermore National Laboratory (LLNL) for testing in PNL facilities. The vendor-supplied chemical and mechanical certifications for these materials are presented in Table 3.1.

The U-bend and SSR specimens were given a variety of heat treatments (solution-annealed and solution-annealed-and-sensitized), then surface-ground to a depth of 0.03 to 0.05 mm (1 to 2 mils) to remove the resulting oxide film before testing. The gauge regions of the SSR specimens were of square cross section of 6.4 mm (0.25 in.)/side and 25.4 mm (1 in.) long. Before testing, the sides of the machined gauge regions of the SSR specimens were tapered slightly by sanding to effect a total width reduction in the center of the gage region of 0.08 to 0.13 mm (3 to 5 mils). The final sanding was done with 220-grit wet/dry paper. The remainder of the specimen was left in the surface-ground condition.

3.2 TUFF ROCK AND TUFF GROUNDWATER

The approximate compositions of the tuff rock and the groundwater (provided by LLNL) are given in Tables 3.2 and 3.3. The rock was obtained from an outcropping of Topopah Spring tuff on the Nevada Test Site and contains soluble salts (Oversby 1984). The composition of the specific lot of rock used in the present study has not been determined, but it is expected to lie within the composition ranges shown in the table. The rock used in these tests was not pretreated (rinsed). Since non-pretreated surface outcroppings contain soluble salts and may increase the composition of Cl^- in solution, these tests are expected to provide conservative results. The water used in the test

TABLE 3.1. Chemical Compositions and Mechanical Properties of Stainless Steel Test Materials

I. Chemical Compositions

Material Code	Material	Alloying Element, wt% C	Mn	Si	P	S	Mo	Ni	Cr	Cu	N
1	Wrought 304L SS sheet	0.017	1.70	0.57	0.019	0.018	0.19	8.66	18.42	0.21	0.082
2	Wrought 304 SS sheet	0.063	1.35	0.45	0.026	0.018	0.10	9.37	18.33	0.19	0.025
3	Wrought 304L SS plate, Heat A	0.024	1.65	0.42	0.031	0.012	--	9.52	18.12	--	--
4	Wrought 304L SS plate, Heat B	0.020	1.81	0.55	0.034	0.004	--	8.55	18.38	--	0.08
5	Wrought 304 SS plate	0.054	1.44	0.39	0.019	0.009	--	8.20	18.07	--	0.048
6	Wrought 316L SS plate	0.020	1.58	0.47	0.029	0.010	2.08	10.68	17.30	0.27	0.065

II. Mechanical Properties (As Received)

Material Code	Material	Yield Strength, ksi	Tensile Strength, ksi	Elongation, %
1	Wrought 304L SS sheet	40.5	84.2	53.0
2	Wrought 304 SS sheet	44.2	90.4	55.5
3	Wrought 304L SS plate, Heat A	42.5	81.1	58.5
4	Wrought 304L SS plate, Heat B	44.2	85.3	58.5
5	Wrought 304 SS plate	47.3	89.4	57.3
6	Wrought 316L SS plate	48.4	84.6	52.0

TABLE 3.2. Percentages of Major Constituents in Topopah Springs Tuff. Fe_2O_3 Represents Total Iron[a]

Constituent	Average Three Analyses, wt%
SiO_2	78.73
Al_2O_3	12.17
Fe_2O_3	0.396
CaO	0.474
MgO	0.123
TiO_2	0.101
Na_2O	4.08
K_2O	3.28
P_2O_5	0.02
MnO	0.052

(a) Schuraytz 1985; Glassley 1986.

was obtained from well J-13, Jackass Flats, Nevada Test Site. The J-13 well water composition noted in Table 3.3 may or may not correspond closely to the composition of the water lying near the ultimate tuff repository location, but it is considered to be reasonably typical of the groundwaters in the region. An indepencent PNL analysis of the J-13 well water obtained for use in the corrosion studies was in substantial agreement with the results of Oversby (1984), as is shown in Table 3.3.

TABLE 3.3. Composition of Water from Well J-13, Jackass Flats, Nevada Test Site

Constituent	Concentration, mg/L[a]	Concentration, mg/L[b]
Na	43.6	46.0
K	5.14	6.5
Mg	1.92	2.1
Ca	12.5	12.9
B	0.122	0.13
Fe	0.006	--
Al	0.012	--
Si	27.0	62
F^-	2.2	2.0
Cl^-	6.5	7.7
HCO_3^-	134	122
SO_4^{-2}	17.5	18.3
NO_2^-	--	1.4
NO_3^-	8.5	7.6
	pH = 7.6	pH = 7.1

(a) As determined by Oversby (1984).
(b) As determined by PNL analysis. (Average of analyses from three barrels of J-13 well water.)

4.0 EXPERIMENTAL PROCEDURES

The experimental work utilized an irradiated autoclave test facility for the irradiated-environment testing of SCC susceptibility; a nonirradiated autoclave for testing of SCC susceptibility under cyclic boil-to-dryness (boil-down) conditions; and a SSR facility for determining susceptibility of the materials to environmentally enhanced crack propagation under dynamic strain conditions. Each facility and the associated operating procedure are described.

4.1 IRRADIATION-CORROSION TESTS

The irradiation-corrosion tests were performed in two Alloy 600 autoclaves placed in a ^{60}Co irradiation facility. The autoclaves were operated at 50°C and 90°C and at (maximum) irradiation intensities of 5×10^5 and 3×10^5 rad/h, respectively. Each autoclave was divided into three zones: water and crushed tuff rock (bottom); crushed rock and air/vapor (middle); and air/vapor only (top). Each zone contained duplicate U-bend specimens of 304 and 304L SS--made from 102-mm x 12.7-mm x 1.5-mm (4-in. x 0.5-in. x 0.060-in.) strips--in both the solution-annealed (15 min at 1050°C) and solution-annealed-and-sensitized (24 h at 600°C) conditions. The U-bend specimens were mounted horizontally on an alumina rod with alumina spacers.

To start the test, the specimen rack was put in place in the autoclave and rock chips were added to cover the desired number (16) of specimens, i.e., two-thirds of the total number (24) of specimens in the autoclave. The autoclave was then sealed, and groundwater (J-13 well water) was added to the autoclave in sufficient quantity to cover the bottom third of the specimens. A temporary sight tube made of transparent plastic tubing connected to the inlet port at the bottom of the autoclave was used to fix the water level at the desired height. The temperature profile within the autoclave was adjusted by appropriate positioning of electrical resistance heaters and insulation on the outside of the autoclave. The temperature within the autoclave was monitored by means of a thermocouple in each of the three distinct environment zones. When the temperature profile was uniform throughout the autoclave, the plastic "sight

tube" was replaced with 3.2-mm (0.125-in.) Alloy 600 feed line tubing, and the autoclave was inserted into the access tube of the irradiation facility for test startup. The autoclaves were operated at atmospheric pressure. During the exposure period, each autoclave was sparged daily via the inlet line with ~240 mL of air to ensure the presence of atmospheric gases within the autoclave. For the first 3 months of testing, the autoclave outlet lines were submerged in a water trap. It was noted, however, that water suck-back would occur in the 90°C test, so the use of water traps was abandoned at that time. The only barrier remaining between the autoclaves and the atmosphere was ~9 m (~30 ft) of 3.2-mm (0.125-in.) tubing.

Problems occurred in the first few days of the 90°C test, due to difficulties in attaining a uniform temperature distribution. The autoclave boiled to dryness and the temperature in the autoclave increased to a maximum of ~120°C for a short time (less than 2 hours). Because this temperature is not high enough to cause metallurgical changes in stainless steel, groundwater was added and the test was continued. The increased concentration of soluble elements resulting from the evaporation of groundwater would be expected to cause the test to be more conservative, i.e., to increase the propensity for SCC to occur. This increased propensity for SCC would most likely be exhibited in the 1-month test results, because the groundwater and rock were changed after the 1-month exposure was completed.

In all cases, the Topopah Spring tuff rock was used in a nominally 6-mm (1/4-in.) major-dimension particle size. The fines resulting from the crushing operation were not discarded, but were included with the larger particles in the autoclave tests. The rock was replaced in each test autoclave (along with the groundwater) after specimen examinations at 1, 3, 5, 7, and 10 months. After the 10-month examination, the rock was not replaced but was reused for the duration of the test. The water, however, was replaced after each specimen examination thereafter, but no water was added during autoclave operation. The water lost to evaporation between specimen examinations was not measured, but was estimated at less than 10% of the total water volume. Typically, a water analysis was made and the U-bend specimen bolts were tightened a fraction of a

turn at each specimen examination. The intent of this tightening was to maintain the high stress in the specimens, which would otherwise be reduced by time-dependent deformation mechanisms.

The irradiation intensity varied somewhat with position within the autoclave because of the length of the autoclave (56 cm or 22 in.) compared with the length of a typical ^{60}Co source (~13 cm or ~5 in.). Also, during the 23- to 25-month test durations, the ^{60}Co irradiation intensity decreased as a natural consequence of radioactive decay. The approximate irradiation intensity as a function of position within each autoclave at the beginning and end of the test is given in Table 4.1. The data given in Table 4.1 were determined using a calibrated ion chamber and thermoluminescent dosimeters. Autoclave attenuation was taken into account.

The irradiation intensities employed in the current tests were purposefully chosen to be higher than any anticipated at the surface of a waste package containing spent fuel under actual repository conditions so that the tests would be performed using conservative values. The desired irradiation intensities were attained by placing each autoclave in an access tube located an appropriate distance from the ^{60}Co sources.

TABLE 4.1. Irradiation Intensity Within Test Autoclaves (rad/h)[a]

Position	50°C Test		90°C Test	
	Test Start	Test End	Test Start	Test End
Top of autoclave	0.82×10^5	0.60×10^5	0.60×10^5	0.45×10^5
Vapor region	1.7×10^5	1.2×10^5	1.2×10^5	0.86×10^5
Vapor/rock region	3.5×10^5	2.6×10^5	2.1×10^5	1.6×10^5
Water/rock region	5.4×10^5	4.0×10^5	2.8×10^5	2.1×10^5
Bottom of autoclave	4.2×10^5	3.1×10^5	2.5×10^5	1.9×10^5

(a) The accuracy is estimated at ±10%.

4.2 BOILDOWN TEST

A groundwater boildown test was used to simulate the possible wetting of the emplaced waste package with subsequent evaporation of some (or all) of the impinging groundwater and deposition of solute residues. Such residues could contain chemical species, such as chlorides, that could promote SCC of the container. The boildown test used an autoclave filled with crushed tuff rock and J-13 well water, with an assemblage of stressed (U-bend) specimens of 304 and 304L SS of various thermal histories embedded in the rock/water matrix. The autoclave was normally operated at 200°C and 1000 psig. Once every 7 days the back pressure on the autoclave was reduced to a value <226 psi and the water was allowed to boil off. After 24 h of "dry" operation, the autoclave was refilled with fresh, air-sparged J-13 well water. Between boildowns, just enough air-sparged water was pumped into the autoclave to ensure that it remained full.

On startup, the tuff rock/specimen array filled the 3.8-L autoclave to within 3.2 cm (1.3 in.) of the top. After the rock and U-bend specimens were in place in the autoclave, 2.23 L of air-saturated J-13 well water was added to fill the autoclave to the top. The autoclave was then sealed, and the test was begun. At each programmed specimen examination, the water in the autoclave at the time of cooldown was reserved and replaced in the autoclave at the time of restart, as was the tuff rock. As in the case of the U-bend specimens in the irradiation-corrosion study, the restraining bolts on the U-bend specimens were tightened a fraction of a turn at each examination.

4.3 SLOW-STRAIN-RATE TESTS

In SSR testing, specimens were strained to failure at a fixed rate while immersed in test environments chosen to simulate sets of repository conditions. The test specimen was enclosed in a heated pressure vessel (autoclave) fitted with a sliding seal for the pull rod. Air-sparged J-13 well water was pumped at a slow rate (~35 mL/h) through the autoclave during the entire test. A bed of crushed tuff rock was placed in the bottom of the autoclave over the water inlet to condition the water before it contacted the test specimen. The water flowed upward, through the crushed rock, over the test specimen, through a

pressure-control valve, and out to drain on a once-through basis during the test. The specimen load and strain were continuously monitored. Strain rates of 10^{-4} in./in.-s and 2×10^{-7} in./in.-s were routinely employed in the present study. The SSR system has been described elsewhere (Westerman et al. 1982).

5.0 RESULTS AND DISCUSSION

The results obtained in the irradiation-corrosion tests, the boildown test, and the SSR tests are presented and discussed in this section.

5.1 IRRADIATION-CORROSION TESTS

At each programmed specimen examination, those specimens showing obvious cracks were removed from the test, while those not showing obvious cracks were replaced in the test autoclaves in their original positions. The 50°C test was concluded after 25 months; the 90°C test, after 23 months. In general, specimens exposed in the rock/vapor and vapor-only regions of the autoclaves showed the most surface corrosion, primarily consisting of patches of red-brown corrosion product. No signs of significant pitting attack were observed on any of the specimens. Specimens exposed in the water/rock regions of the test autoclaves maintained surfaces free of significant corrosion. The appearance of a representative group of specimens at the conclusion of the tests is shown in Figure 5.1. The specimens were not cleaned before being photographed.

The 90°C study had a number of operational problems during its first month of operation. The test autoclave was removed from the irradiated access tube and dismantled four times because of line plugging, i.e., because refreshment air could not be forced into the system, or because of aberrant temperature profile conditions. Each time the autoclave was removed, it was found to be dry, apparently because of moderate overheating accompanied by boiling. The problem was solved by adjusting the position of the control thermocouple, i.e., locating it more closely to the inside wall of the autoclave. The test operated as intended thereafter.

The U-bend failure data are summarized in Table 5.1. Of the 15 total failures observed, 10 occurred in the 90°C test; of these, six were found in the vapor-only region. Also, no failures of 304L SS U-bend specimens were found at 50°C, but four failures of this material were observed at 90°C. Of these, three were located in the vapor-only region. Of the four 304L SS failures and the eleven 304 SS failures, only one specimen of each material was in

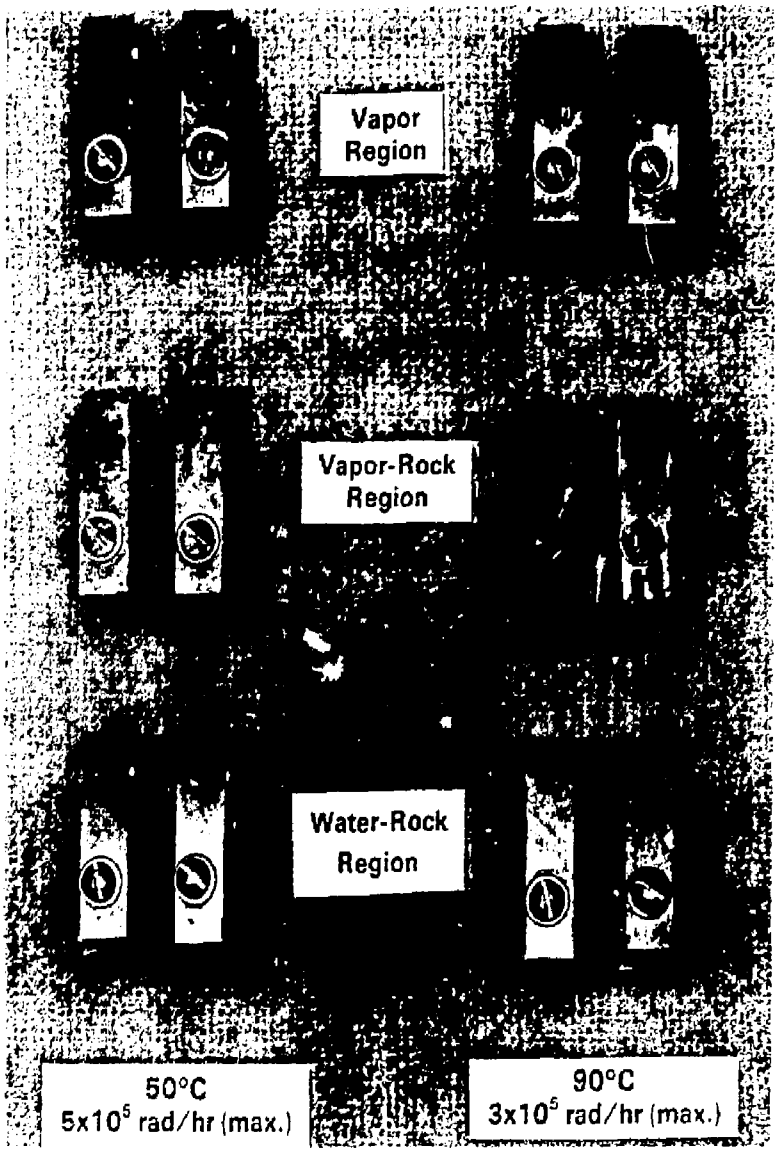

FIGURE 5.1. Appearance of Specimens at Conclusion of Irradiation-Corrosion Tests. Test duration: 25 months, 50°C test; 23 months, 90°C test. Only a representative sample of the test specimens is shown.

TABLE 5.1. Summary of U-Bend Test Data under Irradiation-Corrosion Conditions

Environment	Material Code[a]	Material[b]	50°C Test, 5×10^5 rad/h (max.) Specimen	Failure Time, mo	Failure Mode[c]	90°C Test, 3×10^5 rad/h (max.) Specimen	Failure Time, mo	Failure Mode[c]
Vapor only	1	304L SS SA	P419			P420		
	1	304L SS SAS	P431			P432	10	TG
	2	304 SS SA	P443			P444		
	2	304 SS SAS	P455	1	IG	P456	5	IG
	1	304L SS SA	P421			P422	23	TG
	1	304L SS SAS	P433			P434	14	TG/IG
	2	304 SS SA	P445			P446	23	TG
	2	304 SS SAS	P457	3	IG	P458	3	IG
Rock/vapor	1	304L SS SA	P423			P424		
	1	304L SS SAS	P435			P436	14	TG
	2	304 SS SA	P447			P448		
	2	304 SS SAS	P459	7	IG	P460	3	IG
	1	304L SS SA	P425			P426		
	1	304L SS SAS	P437			P438		
	2	304 SS SA	P449			P450		
	2	304 SS SAS	P461	25	IG	P462		
Rock/groundwater	1	304L SS SA	P427			P428		
	1	304L SS SAS	P439			P440		
	2	304 SS SA	P451			P452		
	2	304 SS SAS	P463	24	IG	P464	1	IG
	1	304L SS SA	P429			P430		
	1	304L SS SAS	P441			P442		
	2	304 SS SA	P453			P454		
	2	304 SS SAS	P465			P466	1	IG

(a) See Table 3.1.
(b) SA = solution annealed (1050°C for 15 min, air cooled).
SAS = solution annealed and sensitized (600°C for 24 h).
(c) D = ductile, TG = transgranular, IG = intergranular.

the solution-annealed condition; all the rest of the failed specimens had been given an additional sensitization heat treatment.

Typically, failed specimens of sensitized 304 SS showed intergranular cracking. Examples of this behavior are shown in Figure 5.2, which shows specimens exhibiting cracks after 1 month in the vapor-only region of the 50°C autoclave and in the water/rock region of the 90°C autoclave.

Four failures were observed in the 304L SS specimens (P432, P422, P434, P436). Of special interest was the failure in the specimen having no sensitization heat treatment (P422), as this material was considered to represent the candidate container material in its most corrosion-resistant condition. The single 304 SS "SA" specimen evidencing failure (P44o) is also of interest, as it was tested in the nonsensitized condition.

Analyses of the water residing in the bottom of the test autoclaves were performed after specimen examinations. The results of these analyses are presented in Table 5.2.

The analyses show a great deal of scatter, with the water showing a very wide range of concentration values of key ingredients, e.g., chloride. Several of the solutions showing high ion strengths were reanalyzed, with the subsequent analyses confirming the initial results. As noted earlier, the rock was not replaced with fresh rock, but fresh J-13 well water was placed in the test with the "old" rock at each specimen examination after 10 months. This procedural change is reflected in the lower ion strengths of the water after 10 months in each test. The chloride concentrations attained high and erratic values prior to this procedure change, apparently reflecting widely varying chloride concentrations in the individual lots of rock.

The following specimens were examined metallographically:

Specimen	Treatment	Time to Failure, mo
P434 (304L SS)	Solution annealed and sensitized	14
P422 (304L SS)	Solution annealed only	23
P446 (304 SS)	Solution annealed only	23

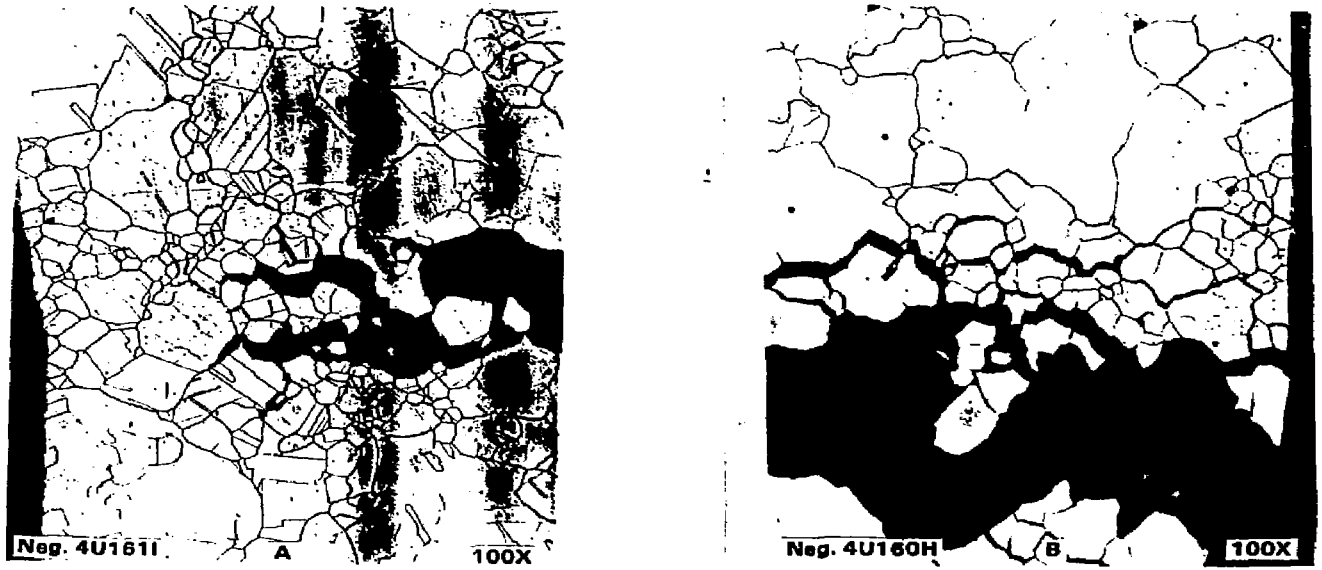

FIGURE 5.2. Intergranular Cracking of Sensitized 304 SS Specimens After 1-Month Exposures in (a) the 50°C Test, Vapor-Only Region (Specimen P455); and (b) the 90°C Test, Rock/Water Region (Specimen P464)

TABLE 5.2. Water Analyses from Irradiation-Corrosion Tests

I. 50°C Test

Time, mo	pH	Conductivity, μmho	Concentration, mg/L F	Cl	NO_2	NO_3	HCO_3	SO_4	Ca	Na	Si	NH_3
3	7.7	780	2.2	51	5	42	190	100	42	110	25	--(a)
5	7.3	5400	7.0	420	570	670	210	970	530	590	47	4.7
7	7.7	6800	7.2	470	680	770	180	1130	560	660	40	11
10	7.7	2520	2.5	119	106	201	142	802	278	218	37	2.0
16	7.8	1926	--(b)	110	24	189	100	510	140	200	26	0.4
24	8.1	2380	--(b)	37	37	323	34.3	806	210	275	37	0.03
25	8.1	1000	--(b)	25	--(c)	125	56.3	219	98	97	28	0.01

II. 90°C Test

Time, mo	pH	Conductivity, μmho	Concentration, mg/L F	Cl	NO_2	NO_3	HCO_3	SO_4	Ca	Na	Si	NH_3
3	9.2	1240	1.5	140	2	1	24	300	23	250	66	--(a)
5	8.2	1085	0.6	14	11	23	65	88	44	27	28	1.4
7	8.0	8450	12	600	1700	110	230	1400	820	950	58	0.3
10	8.3	123	0.2	0.3	3	10	34	8	22	3	22	--(a)
14	8.9	115	0.2	0.6	3	7	33	12	14	7	34	<0.1
23	9.0	601	--(b)	27	43	--(c)	47	138	18	101	28	0.04

(a) No analysis was performed.
(b) Not detected; <0.1 mg/L.
(c) Not detected; <1 mg/L.

All of these specimens were exposed in the vapor-only region of the 90°C irradiation-corrosion test.

Micrographs of Specimen P434 are shown in Figure 5.3. Only transgranular cracking was observed in this specimen, with the exception of a narrow band of material near the specimen surface, where evidence of intergranular corrosion may be seen. This effect may be due to carbon contamination of the stainless steel surface during material processing operations. Abraham et al. (1986)

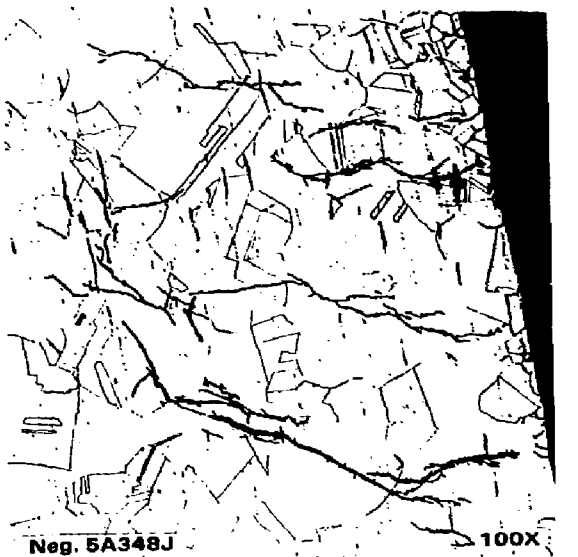

FIGURE 5.3. Transgranular Cracking of Solution-Annealed-and-Sensitized 304L SS (Specimen P434). The specimen was exposed for 14 months to the vapor-only region of the 90°C autoclave test system.

made a similar observation on 304L steel that had been sensitized at 600°C for 100 hours. They attributed the surface carbon to "unavoidable contamination from lubricants during mill operations," and noted that such contamination might enhance the susceptibility of the material to sensitization and SCC.

Specimens P422 and P446 were extensively cracked in the region covered with heavy corrosion products, as is shown in Figure 5.4. Micrographs of the cracked regions of specimens P422 and P446 are presented in Figures 5.5 and 5.6. Both specimens exhibited extensive cracking; only representative regions are shown in the figures. Both specimens cracked in a transgranular fashion, with no evidence of intergranular failure. This cracking failure mode is consistent with the nonsensitized microstructures of the two specimens. These results indicate that in this irradiated tuff/groundwater test environment neither 304 nor 304L SS is completely resistant to cracking, even in the solution-annealed condition, and failure might occur by transgranular or intergranular crack propagation. When failure occurs in nonsensitized 304L SS, it is predominantly transgranular, however.

FIGURE 5.4. Specimens of 304L (Specimen P422) and 304 (Specimen P446) SS After 23-Month Exposure in the 90°C Irradiation-Corrosion Test. Both specimens are extensively cracked in the regions covered with corrosion product.

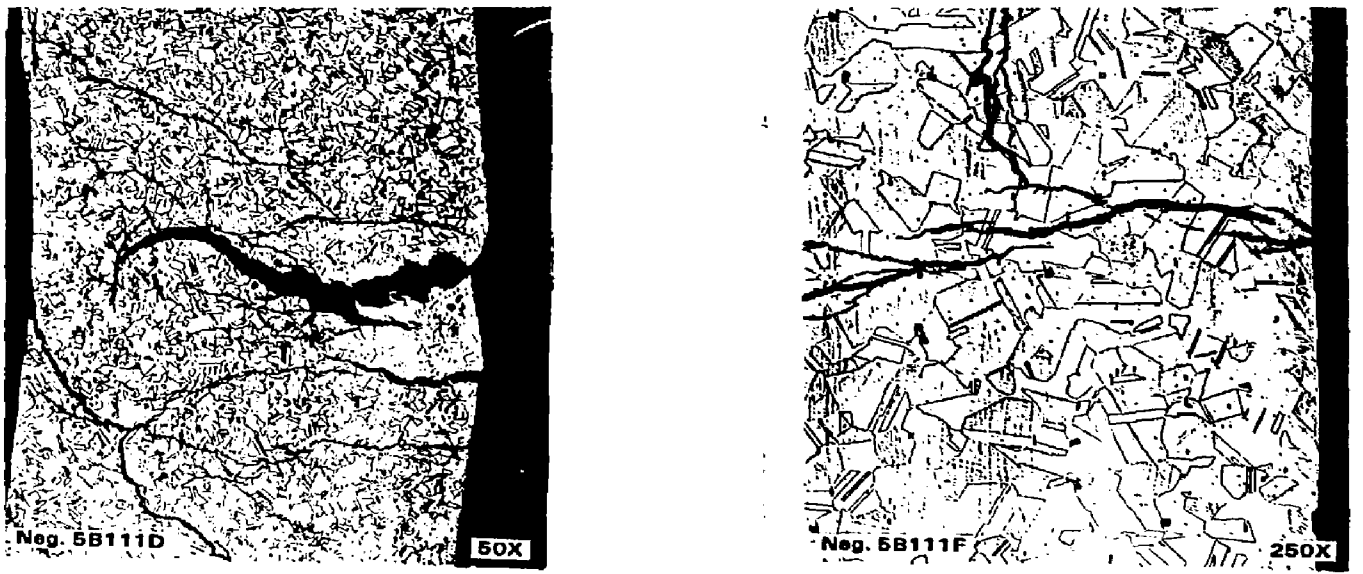

FIGURE 5.5. Transgranular Fracture Mode of Solution-Annealed 304L SS U-Bend (Specimen P422) After 23 Months in the Vapor-Only Region of the 90°C, 3 x 10^5 rad/h Test Autoclave

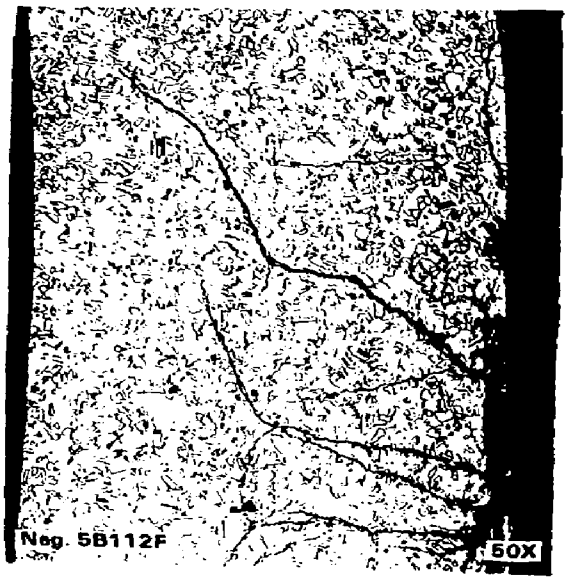

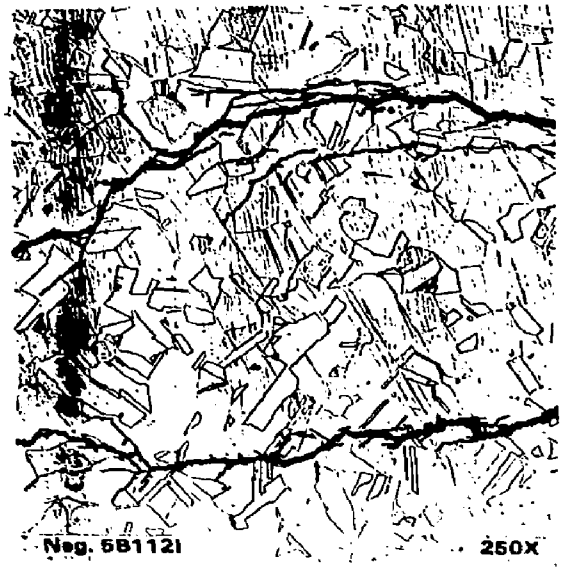

FIGURE 5.6. Transgranular Fracture Mode of Solution-Annealed 304 SS U-Bend (Specimen P446) After 23 Months in the Vapor-Only Region of the 90°C, 3 x 10^5 rad/h Test Autoclave

An effort was made to determine the reasons for the transgranular cracking. Concentration of chloride residues on the surfaces of the specimens during the autoclave exposure, especially on those specimens exposed in the rock/vapor and vapor-only, regions through "wicking" of water to the specimen surfaces via the rock particles or the specimen support structure with subsequent evaporation or through aerosol transport during air sparging, was considered to be a likely factor. Accordingly, one unfailed specimen was selected from each of the three environmental regions in each autoclave for surface analysis.

The specimen surfaces were analyzed by means of x-ray photoelectron spectroscopy (XPS) after removal from the test autoclaves without intermediate cleaning or treatment. In this method, x-ray photons (Mg Kα in the present case) impinge on the surface of a specimen and cause photoelectrons to be emitted. The energy and intensity of the photoelectrons are then analyzed. Elements on the sample surface are identified through their characteristic spectra. The relative intensities of the peaks allow semiquantitative concentration determinations to be made. The results of the analysis are presented in Table 5.3. Approximately three surface monolayers are sampled by the XPS technique, which is capable of detecting chloride in concentrations greater than 0.4 atom percent.

These particular analyses showed no evidence of high concentrations of chlorides building up on the surfaces of the U-bend specimens. The Fe and Ni are most likely derived from the specimen material, while the Ca, Na, Al, and Si are most likely from the rock or groundwater. There were no striking singularities or trends associated with the data that could lead to a straightforward explanation of the U-bend cracking that was observed.

5.2 BOILDOWN TEST

Forty U-bend specimens were initially included in the boildown test. All of the material was given a sensitization heat treatment after a solution anneal. The sensitization heat treatments are listed in Table 5.4.

Nine of the ten 304 SS specimens had failed at the time of the first specimen examination, which took place after 3 months of exposure and

TABLE 5.3. Composition of Surface Layers on U-Bend Specimens

Specimen	Relative Elemental Concentrations, at.%													
	O	C	Ca	Na	F	Fe	Ni	Si	P	Al	S	N	Cl	Cr
P430	56	14	7.5	3.4	1.2	0.4	0.4	10	3.6	2.1	0.9	N.D.[a]	N.D.	N.D.
P462	49	25	3.7	5.5	N.D.	2.4	0.6	7.1	1.9	2.5	(0.7)[b]	N.D.	N.D.	1.6
P444	47	25	0.7	9.1	1.1	0.9	(0.3)	12	0.4	1.3	1.0	1.0	0.6	N.D.
P465	52	24	1.3	2.6	N.D.	1.5	0.8	14	N.D.	1.8	0.7	N.D.	N.D.	0.9
P435	53	21	5.3	0.6	N.D.	0.8	0.4	14	N.D.	1.5	1.2	N.D.	N.D.	0.9
P419	46	34	1.7	1.3	N.D.	1.8	(0.3)	2.6	4.6	2.9	N.D.	3.4	N.D.	1.3

(a) "N.D." indicates that that element was not detected.
(b) An entry in parentheses indicates that although a peak was found at the correct energy for that element, the peak magnitude was not significantly above the noise level.

TABLE 5.4. Sensitization Heat Treatments for Boildown Test

Material Code[a]	Stainless Steel	Sensitization Heat Treatment	Number of Specimens
1	304	24 h at 600°C, air cool	10
2	304L	24 h at 550°C, air cool	10
2	304L	24 h at 700°C, water quench	10
2	304L	8 h at 700°C, water quench	10

(a) See Table 3.1.

15 boildowns. None of the 304L SS specimens showed any sign of cracking at this time, and only a light tarnish film was noted on the specimens. The autoclave underwent an unplanned temperature excursion just before the 6-month specimen examination; it attained a temperature of 290°C for a 41-h period. The autoclave, dry after the forced boildown, was opened for the 6-month specimen examination. No additional failures were noted at this time. The boildown test was terminated after 12 months of exposure and 50 boildowns. At that time, small cracks were noted in the remaining 304 SS U-bend specimen. A metallographic examination revealed intergranular cracking (see Figure 5.7), the anticipated mode of failure of this sensitized material. No failures were observed in any of the 304L SS specimens. Metallographic investigations were conducted on 304L SS specimens having widely different sensitization heat treatments, i.e., 550°C and 700°C for 24 h. Typical microstructures of these specimens are shown in Figure 5.8.

Water analyses from the autoclave were taken under both cold and hot conditions. The results are presented in Table 5.5.

The reason for the lack of concentration of F and Cl after 50 boildowns relative to their concentrations in J-13 well water is not known. While some concentration occurred, it is not enough to account for the 50-fold concentration possible. Formation of insoluble precipitates or reaction products, a mechanical carryover of droplets during boildown by their entrainment in the vapor phase, or solubility of the species in the boildown vapors and subsequent loss from the system are all possibilities.

FIGURE 5.7. Intergranular Cracking Failure of Solution-Annealed-and-Sensitized 304 SS U-Bend After 1-Year Exposure in 200°C Boildown Test (specimen Q330)

Although the boildown test was a severe test for the sensitized 304 SS, it did not prove to be overly severe for the 304L SS, even with the various sensitization heat treatments and the presence of chloride ion and oxygen in the test system. Chemical species capable of promoting intergranular SCC of the sensitized 304 SS were obviously present in the system, but the environment was not sufficiently aggressive to promote inter- or transgranular cracking of the 304L SS during the 1-year duration of the test. In this regard, the system environment was more benign than that in the 90°C irradiation-corrosion test, which promoted cracking of the 304L SS in spite of the generally lower test temperature.

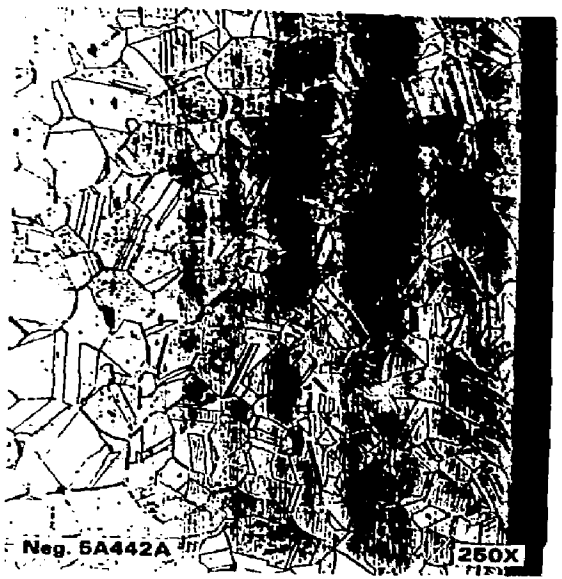

FIGURE 5.8. Solution-Annealed-and-Sensitized 304L SS After 1-Year Exposure in 200°C Boildown Test. No cracking was observed in any 304L SS specimen in this test. The specimen on the left (R085) received a 24-h at 700°C sensitization heat treatment; the specimen on the right (R053) received a 24-h at 550°C sensitization heat treatment.

TABLE 5.5. Water Analyses from Boildown Test

Type of Sample	Concentration, mg/L									
	F	Cl	NO_2	NO_3	SO_4	HCO_3	Ca	K	Na	Si
Cold, at 4 mo	9.4	48	1.7	38	390	160	33	3	269	65
Hot, at 4-1/2 mo	11.4	44	--	36	310	85	13	11	306	315
Cold, at 12 mo	19.0	90	--	38	123	64	7.8	16	205	120

5.3 SLOW-STRAIN-RATE TESTS

SSR tests were performed on 304, 304L, and 316L SS that had undergone a variety of heat treatments. The tests were performed over a wide range of strain rates and environmental conditions. The 304 SS was tested in the mill-annealed and in the solution-annealed-and-sensitized (600°C for 24 h) conditions. The 304L SS was tested in the solution-annealed condition (1050°C for 15 min, water quench) and the solution-annealed-and-sensitized condition (600°C for 10 or 24 h, air cool). The 316L SS was solution annealed at 1000°C for 15 min and water quenched, then heat treated at 250°C for either 1 day or 1 week, followed by a water quench. This heat treatment was chosen because 250°C is the maximum temperature anticipated in the repository. Sensitization of the material was not anticipated. The test data obtained to date are summarized in Tables 5.6 through 5.8.

It is clear from Table 5.6 that solution-annealed 304 SS was ductile at 150°C at all of the strain rates tested. The reduction of area, elongation, yield strength, and ultimate strength were all independent of environment (J-13 groundwater relative to air) and strain rate. The fracture mode was entirely ductile, as shown in Figure 5.9.

Sensitized 304 SS (Table 5.6) was found to be susceptible to intergranular SCC in 150°C J-13 groundwater at strain rates of 2×10^{-7} in./in.-s and 1×10^{-6} in./in.-s; however, no SCC was observed at strain rates of 5×10^{-6} in./in.-s or 1×10^{-4} in./in.-s. The ductility was diminished under the SCC-susceptible conditions, and the fracture mode changed from microvoid coalescence to intergranular fracture. Examples of the fracture morphology are given in Figures 5.10 and 5.11. The fracture was entirely ductile at a strain

TABLE 5.6. Slow-Strain-Rate Test Results for 304 SS[a] at 150°C

I. Mill-Annealed Specimens

Number	Environment	Strain Rate, in./in.-s	Reduction of Area, %	Elongation, %	Yield Strength, ksi	Ultimate Strength, ksi	Failure Mode
P405	Air	1×10^{-4}	80	48	37.4	74.4	Ductile
P406	Air	2×10^{-7}	76	45	35.9	76.6	Ductile
P403	Air	5×10^{-6}	74	46	36.6	75.7	Ductile
P400	Air	5×10^{-6}	73	45	34.0	74.7	Ductile
P395	J-13[b]	5×10^{-6}	79	46	36.8	76.1	Ductile
P396	J-13	5×10^{-6}	68	47	34.5	75.2	Ductile
P397	J-13	1×10^{-4}	78	47	36.1	75.3	Ductile
P404	J-13	1×10^{-4}	80	46	36.3	74.9	Ductile
P401	J-13	2×10^{-7}	76	50	33.5	77.5	Ductile
P402	J-13	2×10^{-7}	76	47	35.1	77.0	Ductile

II. Solution-Annealed and Sensitized[c] Specimens

Number	Environment	Strain Rate, in./in.-s	Reduction of Area, %	Elongation, %	Yield Strength, ksi	Ultimate Strength, ksi	Failure Mode
P413	Air	1×10^{-4}	72	52	21.9	68.0	Ductile
P415	Air	1×10^{-4}	67	52	26.0	68.8	Ductile
P409	Air	5×10^{-6}	73	50	22.4	68.5	Ductile
P417	Air	5×10^{-6}	67	50	18.6	69.9	Ductile
P412	J-13	5×10^{-6}	74	51	20.2	69.3	Ductile
P411	J-13	5×10^{-6}	79	49	21.7	68.6	Ductile
P410	J-13	1×10^{-6}	58	35	19.8	65.5	Intergranular
P407	J-13	1×10^{-4}	76	54	23.5	68.8	Ductile
P408	J-13	1×10^{-4}	75	51	23.5	69.0	Ductile
P414	J-13	2×10^{-7}	51	(d)	22.0	70.1	Intergranular
P416	J-13	2×10^{-7}	26	(e)	20.7	64.5	Intergranular

(a) Material code 5 (see Table 3.1).
(b) "J-13" refers to air-sparged J-13 well water.
(c) Sensitized 24 h at 600°C.
(d) Not determined.
(e) Broke at gage mark.

TABLE 5.7. Slow-Strain-Rate Test Results for 304L SS at 150°C

I. Solution-Annealed Specimens

Number	Environment	Strain Rate, in./in.-s	Reduction of Area, %	Elongation, %	Yield Strength, ksi	Ultimate Strength, ksi	Failure Mode
P379	Air	1×10^{-4}	81	54	28.4	70.1	
P374	Air	1×10^{-4}	78	54	28.6	69.6	
P234[a]	J-13[b]	1×10^{-4}	81	54	25.8	68.4	Ductile
P235[a]	J-13	1×10^{-4}	78	52	27.1	68.2	Ductile
P233[a]	J-13	2×10^{-7}	69	48	28.4	67.7	Ductile
P236[a]	J-13	2×10^{-7}	73	46	26.7	68.2	Ductile
P378[c]	Air	1×10^{-6}	74	48	26.4	69.0	Ductile
P372[c]	Air	1×10^{-6}	79	52	25.9	69.4	Ductile
P382[c]	J-13	1×10^{-6}	69	52	--[d]	--[d]	Ductile
P371	Air	2×10^{-7}	78	54	--[d]	--[d]	Ductile

II. Solution-Annealed and Sensitized Specimens

Number	Environment	Strain Rate, in./in.-s	Reduction of Area, %	Elongation, %	Yield Strength, ksi	Ultimate Strength, ksi	Failure Mode
P243[e]	Air	1×10^{-4}	74	49	29.4	68.6	Ductile
P239[e]	J-13	1×10^{-4}	72	50	--[d]	--[d]	Ductile
P240[e]	J-13	1×10^{-4}	75	52	29.6	69.1	Ductile
P241[e]	J-13	2×10^{-7}	76	49	26.6	68.8	Ductile
P244[e]	J-13	2×10^{-7}	70	48	27.2	68.8	Ductile
P384[f]	Air	1×10^{-6}	72	53	19.3	64.6	Ductile
P393[f]	Air	1×10^{-6}	69	50	20.4	63.9	Ductile
P387[f]	J-13	1×10^{-6}	57	51	21.5	65.1	Ductile
P385[f]	J-13	1×10^{-6}	70	53	20.6	65.4	Ductile
P389	Air	2×10^{-7}	78	50	--[d]	--[d]	Ductile

(a) Specimens P233 through P244 are from heat A (material code 3, Table 3.1).
(b) Air-sparged J-13 well water.
(c) Specimens P371 to P394 are from heat B (material code 4, Table 3.1).
(d) Not determined because of equipment malfunction.
(e) Sensitized 10 h at 600°C, air cooled.
(f) Sensitized 24 h at 600°C, air cooled.

rate of 5×10^{-6} in./in.-s (Figure 5.10) but was entirely intergranular at a strain rate of 1×10^{-6} in./in.-s (Figure 5.11).

No SCC was observed in 304L SS at 150°C (Table 5.7). The fracture mode was ductile in each case. Examples of the fracture morphology are given in Figure 5.12.

TABLE 5.8. Slow-Strain-Rate Test Results for 304[a] and 316L[b] SS at 95°C and a Strain Rate of 1×10^{-6}/s

I. 304 SS

Specimen Number	Environment	Sensitization Heat Treatment	Reduction of Area, %	Elongation, %	Yield Strength, ksi	Ultimate Strength, ksi	Failure Mode
151	Air	1 wk at 700°C, WQ[c]	57	34	66.2	91.7	Ductile
152	Air	1 wk at 700°C, WQ	56	33	70.8	91.5	Ductile
153	J-13[d]	1 wk at 700°C, WQ	57	35	68.3	89.9	Ductile
154	J-13	1 wk at 700°C, WQ	62	34	69.0	90.4	Ductile

II. 316L SS

Specimen Number	Environment	Sensitization Heat Treatment	Reduction of Area, %	Elongation, %	Yield Strength, ksi	Ultimate Strength, ksi	Failure Mode
121	Air	1 day at 250°C, WQ	54	17	101.1	106.1	Ductile
122	J-13	1 day at 250°C, WQ	56	16	100.9	106.5	Ductile
123	J-13	1 day at 250°C, WQ	54	16	100.8	107.8	Ductile
124	J-13	1 day at 250°C, WQ	53	16	100.6	106.4	Ductile
125	Air	1 day at 250°C, WQ	54	16	97.0	107.2	Ductile
132	J-13	1 wk at 250°C, WQ	47	12	109.5	114.5	Ductile
133	Air	1 wk at 250°C, WQ	51	13	111.6	117.0	Ductile
134	Air	1 wk at 250°C, WQ	48	13	105.7	113.1	Ductile
135	J-13	1 wk at 250°C, WQ	47	13	106.2	112.3	Ductile

(a) Material code 5 (see Table 3.1). These specimens were not solution annealed.
(b) Material code 6 (see Table 3.1).
(c) Water quench.
(d) Air-sparged J-13 well water.

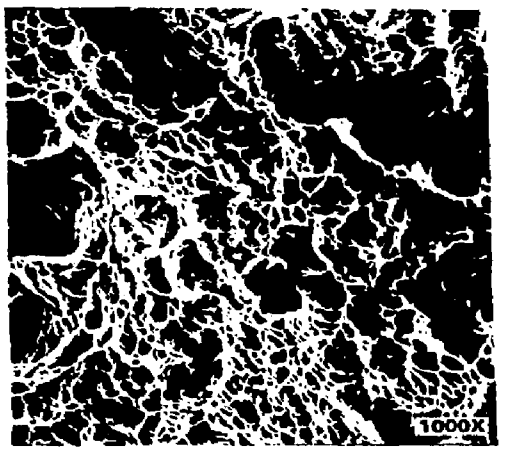

FIGURE 5.9. Fracture Surface of Solution-Annealed 304 SS Specimen (P395) Strained to Failure in 150°C J-13 Well Water at a Strain Rate of 5×10^{-6}/s

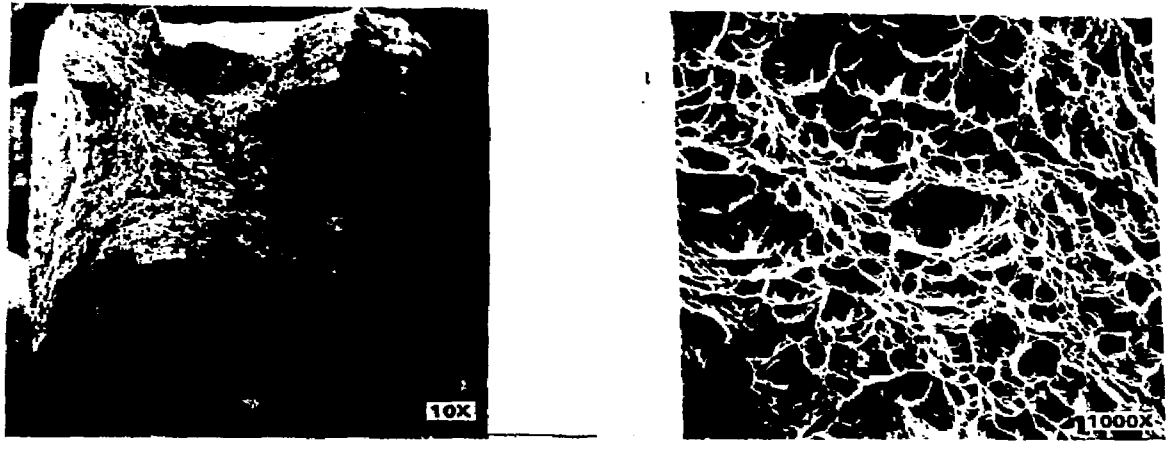

FIGURE 5.10. Fracture Surface of Solution-Annealed-and-Sensitized 304 SS Specimen (P411) Strained to Failure in 150°C J-13 Well Water at a Strain Rate of 5×10^{-6}/s

FIGURE 5.11. Fracture Surface of Solution-Annealed-and-Sensitized 304 SS Specimen (P410) Strained to Failure in 150°C J-13 Well Water at a Strain Rate of 1 x 10^{-6}/s

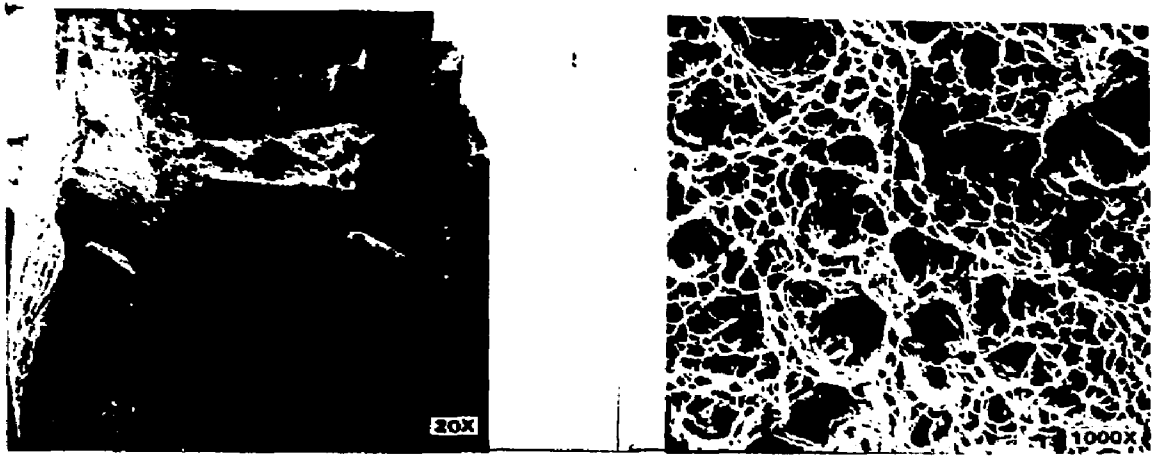

FIGURE 5.12. Fracture Surface of a Solution-Annealed-and-Sensitized 304 SS Specimen (P240) Strained to Failure in 150°C J-13 Well Water at a Strain Rate of 1×10^{-6}/s

Neither 304 SS nor 316L SS exhibited susceptibility to SCC at 95°C (Table 5.8). The ductility of the 316 SS was considerably lower than that of the other materials tested; however, this is consistent with a greater amount of cold work in the as-received material. Examples of the ductile fracture morphology are given in Figure 5.13 (304 SS) and Figure 5.14 (316L SS). There was no evidence that the heavy cold work in the material assisted in producing a sensitized microstructure.

5.4 SENSITIZATION STUDY

A study was done to correlate microstructural changes during sensitization treatment with the results of SSR tests and nondestructive measures of sensitization. This study consisted of metallographic and electron microscopic analyses of the microstructure and electrochemical potentiokinetic reactivation (EPR) measurement of the degree of sensitization.

The EPR test is a rapid, quantitative, and nondestructive measurement of the degree of sensitization. It is based on the charge transfer between the metal and electrolyte during reactivation from the passive state. In nonsensitized material, the passive film remains intact for longer times during reactivation and the anodic peak is suppressed. This allows an easy distinction between sensitized and nonsensitized material. The result of this test, the EPR number, is expressed in coulombs/cm^2 of exposed surface. Values over 2 or 3 indicate a sensitized microstructure. The test is repeated three times for each specimen. The second test is done on the same area as the first test; the result is generally higher than that of the first test if the microstructure is sensitized. The third test is done on a new area to confirm the result of the first test.

The results of EPR tests of 304, 304L, and 316L SS specimens are given in Table 5.9. It is clear that 304 SS was sensitized by heating to 600°C for 24 h but that no sensitization was present after heating to 700°C for 168 h. This is consistent with the results of the SSR tests, where reduced ductility and intergranular fracture were observed in specimens heated to 600°C but not in specimens heated to 700°C.

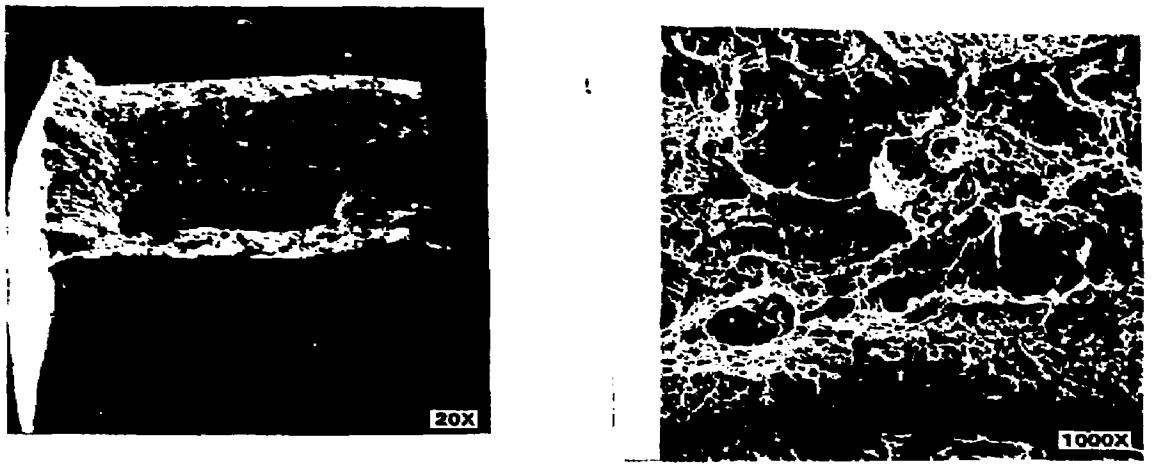

FIGURE 5.13. Fracture Surface of a Solution-Annealed-and-Sensitized (168 h at 700°C) 304 SS Specimen (153) Strained to Failure in 95°C J-13 Well Water at a Strain Rate of 1 x 10^{-6}/s

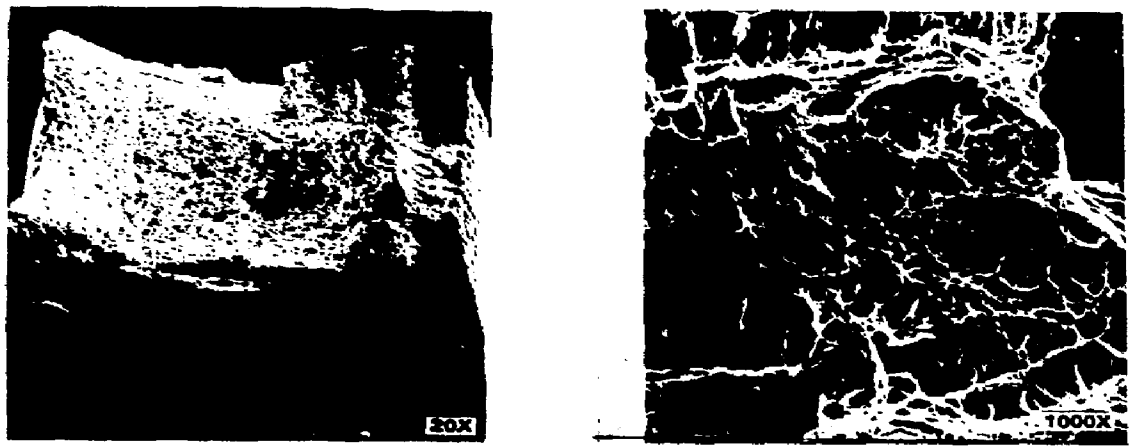

FIGURE 5.14. Fracture Surface of a Solution-Annealed-and-Sensitized (168 h at 250°C) 316L SS Specimen (135) Strained to Failure at 1 x 10^{-6}/s

TABLE 5.9. Results of Electrochemical Potentiokinetic Reactivation Tests

Material Code	Specimen Number	Heat Treatment	ASTM Grain Size No.	EPR Number 1	2	3
		I. 304 SS Mill-Annealed Specimens				
5	P395		7	0.00	0.00	0.00
5	P396		7	0.00	0.00	0.00
		II. 304 SS Solution-Annealed-and-Sensitized Specimens				
5	P407	600°C/24 h	1	38.94	48.79	23.12
5	P409	600°C/24 h	1	13.82	40.16	--
5	151	700°C/168 h	6	0.00	0.00	0.39
5	153	700°C/168 h	6	0.00	0.00	0.00
		III. 304L SS Solution-Annealed Specimens				
3	P233		5	0.00	0.00	0.00
3	P234		5	0.00	0.00	0.00
		IV. 304L SS Solution-Annealed-and-Sensitized Specimens				
3	P239	600°C/10 h	4	37.82	50.28	33.52
3	P240	600°C/10 h	4	25.35	42.11	21.92
4	P384	600°C/24 h	4	1.42	0.00	0.69
		V. 316L SS Solution-Annealed-and-Sensitized Specimens				
6	121	250°C/24 h	4	0.00	0.00	0.00
6	122	250°C/24 h	4	0.00	0.00	0.00
6	132	250°C/168 h	4	0.00	0.00	0.00
6	133	250°C/168 h	4	0.00	0.00	0.00

(a) See Table 3.1.

The EPR tests indicate that 304L SS was sensitized after heating to 600°C for 10 h, but that most of the sensitization was gone after heating to 600°C for 24 h. This is consistent with the observations from metallographic and TEM analyses that a continuous grain boundary precipitate was formed after 10 h but

that the precipitate was not present after 24 h. Neither heat treatment produced a reduction of ductility or a change in the nature of the fracture surface in SSR tests.

The 316L SS was not sensitized by heating to 250°C for 24 or 168 h. This fact is demonstrated by the results of the EPR tests, SSR tests, fractography, and metallography.

The results of metallography of 304 SS are given in Figures 5.15 to 5.17. A mill-annealed specimen (Figure 5.15) was found to have carbide precipitates dispersed throughout the microstructure. The grain boundaries were essentially free of precipitates. The microstructure of a specimen sensitized for 24 h at 600°C is shown in Figure 5.16. Continuous precipitates were found at the grain boundaries. A specimen sensitized at 700°C for 168 h was found to have large, discontinuous grain boundary precipitates, as shown in Figure 5.17.

The microstructure of 304L SS was altered by sensitization at 600°C, as is shown in Figures 5.18 and 5.19. The solution-annealed microstructure (Figure 5.18) had no grain boundary precipitation, but the sensitized microstructure had a continuous grain boundary precipitate (Figure 5.19).

The microstructure of the 316L SS (Figure 5.20) was typical of a cold-worked material. There was no evidence of grain boundary precipitation during the sensitization treatment of 168 h at 250°C, although large precipitates were found throughout the microstructure.

Two specimens of 304 SS were studied using transmission electron microscopy (TEM). One specimen was heated to 600°C for 24 h and had heavily decorated grain boundaries, indicating a sensitized condition (Figure 5.21). The other specimen was heated to 700°C for 168 h. This heat treatment produced a microstructure with coarse, discontinuous precipitates along the grain boundaries (Figure 5.22).

Three specimens of 304L SS were studied using TEM: a solution-annealed specimen, a specimen heated to 600°C for 10 h, and a specimen heated to 600°C for 24 h. Neither the solution-annealed specimen (Figure 5.23) nor the specimen heated to 600°C for 24 h (Figure 5.24) showed any grain boundary precipitation, but the specimen heated to 600°C for 10 h had a continuous grain

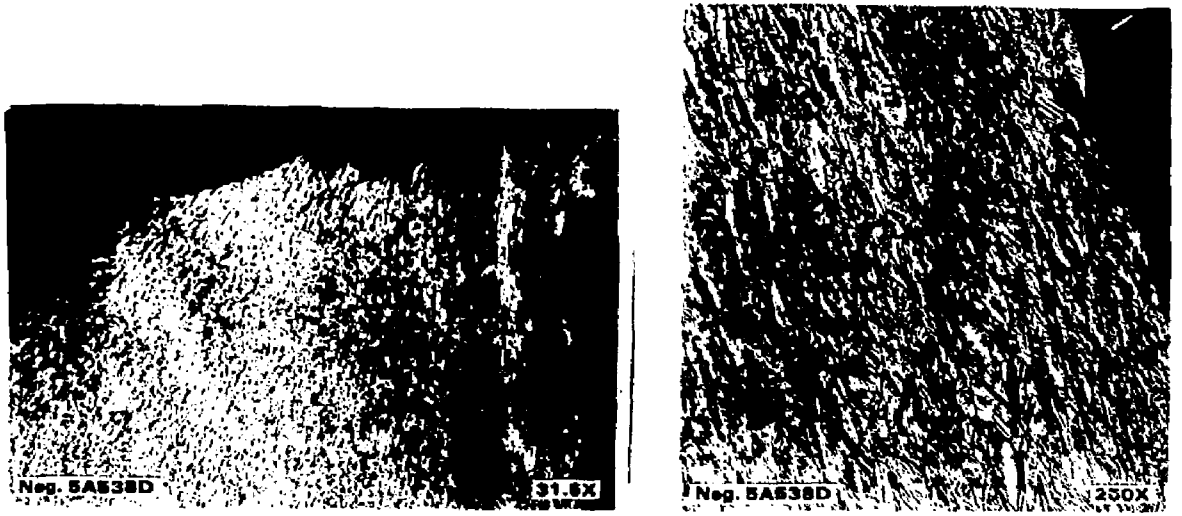

FIGURE 5.15. Microstructure of Solution-Annealed 304 SS Specimen (P396)

FIGURE 5.16. Microstructure of Solution-Annealed 304 SS Specimen (P409) Sensitized at 600°C for 24 h

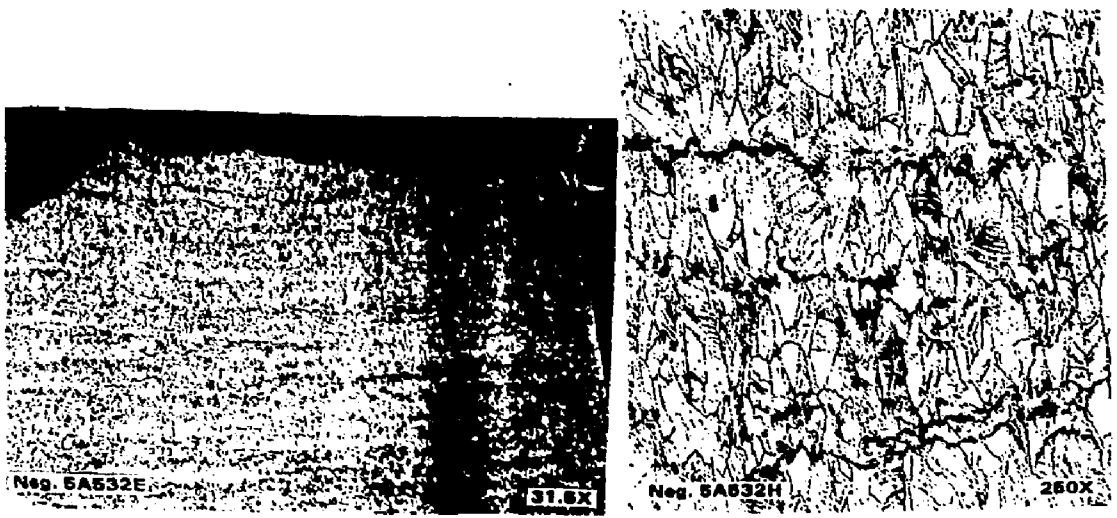

FIGURE 5.17. Microstructure of Solution-Annealed 304 SS Specimen (15J) Sensitized at 700°C for 168 h

FIGURE 5.18. Microstructure of Solution-Annealed 304L SS Specimen (P384)

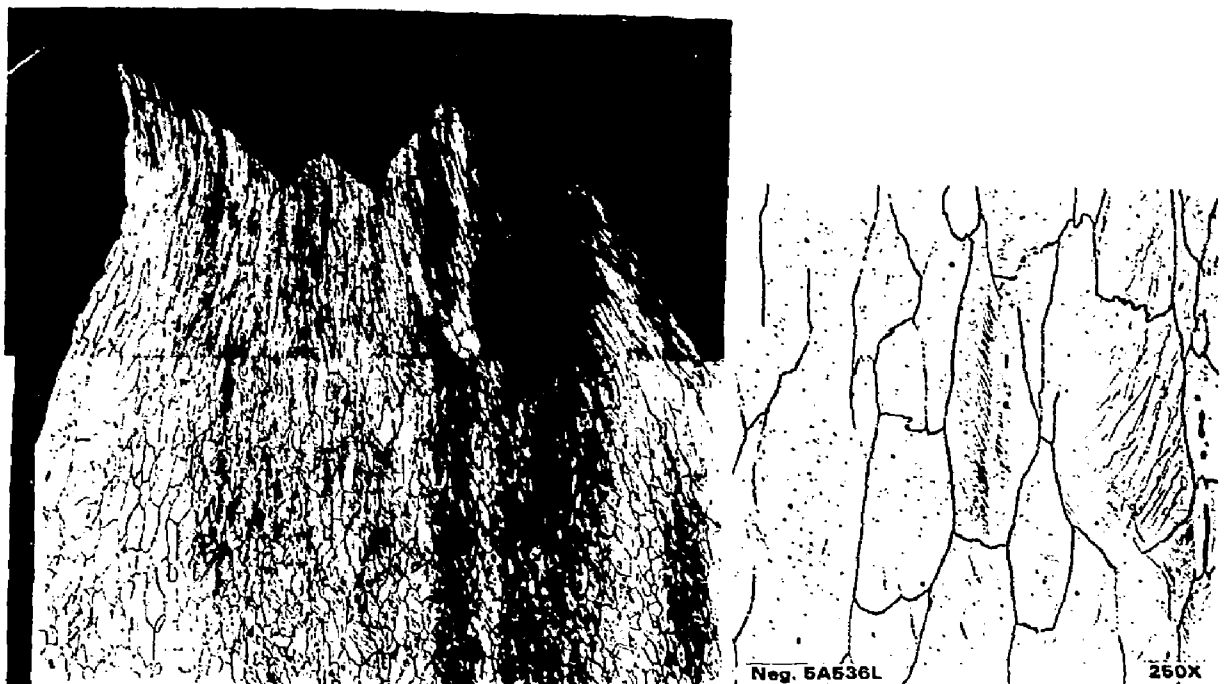

FIGURE 5.19. Microstructure of Solution-Annealed 304L SS Specimen (240) Sensitized at 600°C for 10 h

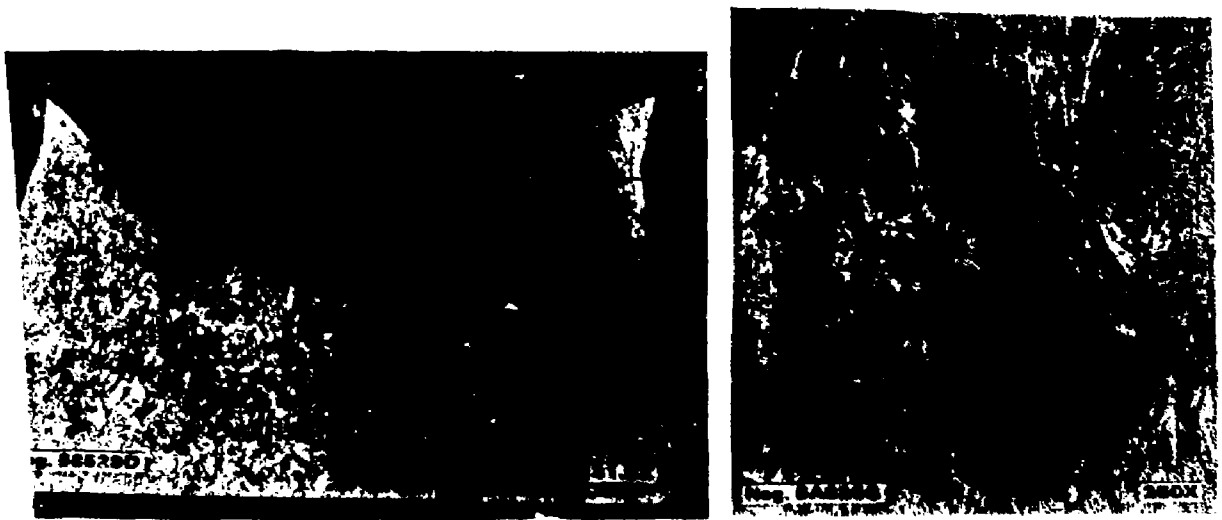

FIGURE 5.20. Microstructure of 316L SS Specimen (133) Cold Worked and Heated to 250°C for 168 h

FIGURE 5.21. TEM Micrograph of 304 SS Specimen (P407) Solution-Annealed and Sensitized at 600°C for 24 h

FIGURE 5.22. TEM Micrograph of 304 SS Specimen (153) Heated to 700°C for 168 h

FIGURE 5.23. TEM Micrograph of Solution-Annealed 304L SS Specimen (P233), Showing Clean Grain Boundaries at Triple Point

FIGURE 5.24. TEM Micrograph of 304L SS Specimen (P334) Solution-Annealed and Heated to 600°C for 24 h, Showing Clean Grain Boundaries at Triple Point

boundary precipitate (Figure 5.25). No explanation for this anomalous behavior has been found except that the specimens were fabricated from two different heats of material, and perhaps some irregularity in the processing of the steel increased the sensitization kinetics of the specimens that were heated to 600°C for 10 h.

Two specimens of 316L stainless steel were examined using TEM. Both specimens were given a 250°C heat treatment; one for 24 h and one for 168 h. Neither specimen had grain boundary precipitates (Figures 5.26 and 5.27).

FIGURE 5.25. TEM Micrograph of 304L SS Specimen (P239) Solution-Annealed and Heated to 600°C for 10 h, Showing Precipitate Formation at the Grain Boundary

FIGURE 5.26. TEM Micrograph of 316L SS Specimen (122) Heated to 250°C for 24 h, Showing Clean Grain Boundaries and Triple Point

FIGURE 5.27. TEM Micrograph of 316L SS Specimen (133) Heated to 250°C for 168 h, Showing Clean Grain Boundaries and Triple Point

6.0 CONCLUSIONS

The following conclusions are based on the results of the irradiation-corrosion, boildown, and SSR testing:

- Under gamma flux and stress conditions that are accelerated with respect to the expected case for the repository, it was found that solution heat treated 304L can exhibit transgranular stress corrosion cracking. It is likely that the cracking was chloride induced and accelerated by additional oxidizing power resulting from the gamma flux. No cracking was found in this material without gamma flux. Sensitized 304L exhibited stress corrosion cracking both with and without gamma flux.

- Most of the failures observed in the gamma flux test occurred in the vapor-phase region of the 90°C autoclave test. The test conditions differ from the anticipated repository conditions because 1) the temperature was not well controlled at the beginning of the 90°C test, and boildown occurred; 2) the rock used in the test was surface outcropping, containing soluble salts; 3) the method of air-sparging might have caused the transfer and concentration of chlorides on the specimen surfaces; 4) the gamma radiation doses were higher than expected; and 5) the applied stress was quite high.

- Type 304 stainless steel was more susceptible to stress corrosion cracking than 304L in that cracking of solution heat treated Type 304 occurred over a broader temperature range when exposed to gamma flux. When gamma flux was not present, the sensitized 304 exhibited intergranular stress corrosion cracking while the sensitized 304L did not.

- The 304 SS was found to be susceptible to intergranular SCC in SSR tests performed in 150°C J-13 well water after sensitization at 600°C for 24 h. The SCC was found to be most severe when tests were done at a strain rate of 2×10^{-7} in./in.-s, but cracking was also observed at 1×10^{-6} in./in.-s. SCC was not detected at higher strain rates.

- The susceptibility of 304 SS to SCC in SSR tests was correlated with the formation of grain boundary precipitates. Cracking was intergranular in all cases.
- Neither 304L nor 316L SS was found to be susceptible to SCC in SSR tests using a J-13 well water test environment. The 304L SS was tested at 150°C, and the 316L SS was tested at 95°C. The 304L material was found to be sensitized after heating to 600°C for 10 h, but the width of the chromium-depleted zone near the grain boundaries was probably too small to induce cracking in these tests in a relatively benign environment.

7.0 REFERENCES

Abraham, T., H. Jain, and P. Soo. 1986. Stress Corrosion Cracking Tests on High-Level-Waste Container Materials in Simulated Tuff Repository Environments. NUREG/CR-4619, prepared for the U.S. Nuclear Regulatory Commission by Brookhaven National Laboratory, Upton, New York.

Beavers, J. A., N. G. Thompson, and R. N. Parkins. 1985. "Stress Corrosion Cracking of Low Strength Carbon Steels in Candidate High Level Waste Repository Environments: Environmental Effects." Nuclear and Chemical Waste Management Vol. 5, pp. 279-296.

Glassley, W. E. 1986. Reference Waste Package Environment Report. UCRL-53726, Lawrence Livermore National Laboratory, Livermore, California.

LaQue, F. L., and H. R. Copson, ed., Corrosion Resistance of Metals and Alloys, Second Edition, Chapter 15, Reinhold Publishing Co., New York (1963).

McCright, R. D., H. Weiss, M. C. Juhas, and R. W. Logan. 1983. Selection of Candidate Canister Materials for High-Level Nuclear Waste Containment in a Tuff Repository. UCRL-89988, Lawrence Livermore National Laboratory, Livermore, California.

O'Neal, W. C., D. W. Cregg, J. N. Huckman, E. W. Russell, and W. Stein. 1984. Preclosure Analysis of Conceptual Waste Package Designs for a Nuclear Waste Repository in Tuff. UCRL-53595, Lawrence Livermore National Laboratory, Livermore, California.

Oversby, V. M. 1984. Reaction of Topopah Spring Tuff with J-13 Well Water at 90°C and 150°C. UCRL-53552, Lawrence Livermore National Laboratory, Livermore, California.

Payer, J. H., W. E. Berry, and W. K. Boyd. 1976. "Constant Strain Rate Technique for Assessing Stress-Corrosion Susceptibility." Stress Corrosion--New Approaches. ASTM STP 610, American Society for Testing and Materials, Philadelphia, Pennsylvania, pp. 82-93.

Schuraytz, B. 1985. Geochemical Gradients in the Topopah Spring Member of the Paintbrush Tuff: Evidence for Eruption Across a Magmatic Interface. UCRL-53698, Lawrence Livermore National Laboratory, Livermore, California.

Westerman, R. E., S. G. Pitman, and J. L. Nelson. 1982. General Corrosion, Irradiation-Corrosion, and Environmental-Mechanical Evaluation of Nuclear Waste Package Structural Barrier Materials. PNL-4364, Pacific Northwest Laboratory, Richland, Washington.

Winograd, I. J. 1971. "Hydrogeology of Ash-Flow Tuff: A Preliminary Statement." Water Resources Research I (4):994-1006.

Wolfsberg, K., and B. R. Erdal. 1981. Research and Development Related to Nevada Nuclear Waste Storage Investigations, October-December 1980. LA-8739-PR, Los Alamos Scientific Laboratory, Los Alamos, New Mexico.